The Effect of Neutrals on the Global Heliosphere and Interplanetary Shock Propagation Time to the Heliopause

P. C. Liewer
Jet Propulsion Laboratory, California Institute of Technology, Pasadena, CA 91109

S. Roy Karmesin
Department of Applied Mathematics, California Institute of Technology, Pasadena, CA 91125

J. U. Brackbill
Los Alamos National laboratory, Los Alamos, NM 87545

Abstract

A two-dimensional time-dependent two-fluid hydrodynamic model has been used to study numerically the effect of interstellar neutrals on the size and structure of the heliosphere. The interstellar neutrals, coupled to the plasma by charge-exchange collisions, lead to a draruatic decrease in the size of the heliosphere - 30% for the parameters studied. We find that a build up of neutral hydrogen in front of the leading edge of the heliosphere, seen in earlier models, occurs only when the flow in the interstellar medium is supersonic. When the flow is subsonic, no such hydrogen "wall" is seen in the simulations, suggesting that the distribution of scattered solar H Ly α light may be quite different for this case. We "have also calculated the propagation] of an interplanetary shock to the heliopause as a possible trigger for the 1992 Voyager 2-3 kHz radio emission event. We find that the interstellar plasma density, observed emission cut-off frequency, and heliopause location can all be made consistent once the effect of the reduction in the size of the heliosphere by the interaction with the neutrals is included.

Introduction

The effects of the interstellar neutrals on the size and structure of the global heliosphere has been modeled by several groups (*Baranov and Malama*, 1993 and references therein; *Pauls* et al., 1995 and these proceedings). Using a two-dimensional steady-state model, *Baranov and Malama* (1993, hereafter B&M) showed that neutrals, coupled to the plasma by charge-exchange collisions, led to a significant decrease in the size of the heliosphere, e.g., the heliopause moved in from 250 AU to about 170 AU when a neutral density $n_N = 0.14\, cm^{-3}$ was assumed. The model used by B&M treats the plasma as a fluid and the neutrals as particles with source terms coupling the plasma and neutrals. A Monte Carlo technique was used to compute the neutral atom trajectories. A steady state solution was achieved by iterating between the kinetic neutral and hydrodynamic plasma calculations.

We have developed a two-dimensional time-dependent hydrodynamic model which treats both the neutral and plasma components as fluids, allowing us to study dynamic problems such as interplanetary shock propagation to the heliopause. Since the neutral mean-free path can be comparable to the length scales in this problem, the accuracy of a fluid treatment of neutrals can be questioned. However, iterating between a Monte Carlo neutral computation and a fluid plasma computation at every time step of a time-dependent code would be too costly.

Using our two-fluid neutral-plasma model with the parameters in B&M, we recover their results for a "two shock" heliosphere, that is, a heliosphere with a bow shock upstream of the leading edge of the heliopause created by the supersonic interstellar flow. As seen by B&M, the size of the heliosphere decreases dramatically and we observe a build up of neutrals at the leading edge or "nose" of the heliosphere between the bow shock and the heliopause. At present, it not known whether or not the heliosphere has a bow shock. Since the magnetic field in the very local interstellar medium (VLISM) cannot be measured, it is not known whether the flow is above or below the fast magnetosonic speed. When we use parameters such that the VLISM flow is subsonic, a case not studied by B&M, we find that no such abrupt increase in neutral hydrogen forms at the leading edge or nose of the heliosphere which may have implications for the distribution of scattered solar H Lyman α radiation. A similar decrease in the size of the heliosphere is observed in this "one shock" case.

This two-fluid plasma-neutral model has also been used to study the propagation of an interplanetary shock to the heliopause which has been suggested as a possible trigger for the 2-3 kHz emissions detected by the Voyager spacecraft in 1992 (*Gurnett* et al., 1993). The propagation of an interplanetary shock to the heliopause has been modeled previously by *Steinolfson and Gurnett* (1995) using a two-dimensional time-dependent hydrodynamic model. We have extended these calculations by using a model which also includes the charge-exchange interaction between tile plasma and the interstellar neutral hydrogen and find that the interstellar plasma density, observed emission cut-off frequency and heliopause location can all be made consistent once the effect of the reduction in the size of the heliosphere by the interaction with the neut rals is included. By assuming a VLISM neutral density of 0.14 cm^{-3}, the IP shock propagation time agrees with the time suggested by the observations (about 400 days) when the VLISM has a density of only $n_p = 0.04\ cm^{-3}$, corresponding to a 1.8 kHz cutoff frequency, which is the lowest frequency seen in the Voyager emission spectra.

Numerical Model

The model used in this work is a time-dependent two-dimensional two-fluid hydrodynamic model. This is similar to the hydrodynamic model used previously by *Karmesin* et *al.* (1995) to study the motion of the termination shock in response to solar-cycle variations in the solar wind ram pressure. The neutral-plasma charge-exchange coupling terms are taken from *Holzer* (1972) with the resonant charge-exchange cross section used in B&M and *Baranov* et *al.* (1991). '1'bus, we solve the equations for each species [$i, j =$ p (plasma) or N (neutrals)]:

$$\frac{\partial n_i}{\partial t} + \nabla \cdot n_i\vec{v}_i = S_{j\to i} - S_{i\to j}$$

$$\frac{\partial n_i\vec{v}_i}{\partial t} + \nabla \cdot n_i\vec{v}_i\vec{v}_i - \nabla p_i = \vec{R}_{j\to i} - \vec{R}_{i\to j}$$

$$\frac{\partial e_i}{\partial t} + \nabla \cdot \vec{v}_i\,(e_i + p_i) = Q_{j\to i} - Q_{i\to j}$$

where $e_i = p_i/(\gamma - 1) + \frac{1}{2}n_i m v_i^2$ is the total energy, m is the mass, and $\gamma = 5/3$. The plasma-neutral coupling terms are

$$S_{j\to i} = n_i n_j \sigma_{cx} u^*$$

$$\vec{R}_{j\to i} = n_i n_j \vec{v}_j \sigma_{cx} u^*$$

$$Q_{j\to i} = n_i e_j \sigma_{cx} u^*$$

where $\sigma_{cx} = (a - b\ln u)^2\ cm^2$ with $a = 1.64 \times 10^{-7}$, and $b = 6.95 \times 10^{-9}$, where u is the relative velocity between the neutrals and plasma ions in cm/s; and where the effective velocity is $u^* = \left(\frac{128k_B}{9\pi m}(T_p + T_N) + (u - u_N)^2\right)^{1/2}$ with T_p and T_N equal to the proton and neutral temperatures respectively (*Baranov et al.*, 1991). These are the equations solved for the plasma and neutral species outside the heliopause. The charge-exchange interaction between protons and neutral hydrogen leaves the total number of each species unchanged and thus, in general, there would be no sources or sinks in the continuity equations ($S_{j\to i} = S_{i\to j}$). However in our model, as in *Pauls* et *al.* (1995), the very energetic neutrals which are created by charge exchange *inside* the heliopause are neglected, e.g., they are not incorporated into the neutral fluid inside the heliopause. These "solar wind" energetic neutrals form a new non-thermal population) of neutrals inside tile heliopause with a much longer mean-free path. Therefore, neglecting these energetic neutrals, the $S_{p\to N}$, $\vec{R}_{p\to N}$ arid $Q_{p\to N}$ terms arc set to zero in the equations for the neutrals only inside the heliopause and the neutral fluid loses particles, momentum arid energy to the solar wind plasma. The heliopause is easily located during the simulations by monitoring the plasma specific internal energy $i = k_B T/(\gamma - 1) + mv^2/2$ which changes by more than a factor of 100 across the heliopause.

Effects of Neutrals on the Size and Structure of the Heliosphere

In this section results are presented from four simulations illustrating the effects of the neutral-plasma charge-excJlarlgc coupling on the size of the heliosphere and on the neutral distribution itself.

Simulation Results for a Two Shock Heliosphere

Simulation results from a case without neutrals (Case 1, dashed line) and a case with neutrals (Case 2, solid line), with other parameters the same, are compared in Fig. 1. I'lotted are density and velocity profiles along a line from the inner grid boundary through the nose of the heliosphere, e.g., along the upstream symmetry axis of our 2D grid ($\theta = 0$). The parameters for Case 1 are those used by B&M. For the solar wiud plasma at 1 AU, $n_p = 7\ cm^{-3}$, $v_{vsw} = 450\ km/s$, arid $T_p = 1.5 \times 10^5$ K; for the VLISM plasma, $n_p = 0.07\ cm^{-3}$, $v_{vlism} = 25\ km/s$ and $T_p = 10^4$ K. Case 2 has the same parameters except there is also a neutral component with density $n_N = 0.14\ cm^{-3}$ which has the same velocity and temperature as the interstellar plasma. It can be seer L in Fig. 1 that the heliosphere is dramatically smaller when the charge-excharlge coupling between the neutrals and the plasma is included. The termination shock (seen as first the abr upt increase in density) has decreased to 115 AU in Case 2 from 170 AU in Case 1 and the heliopause (the second abrupt increase in density) has decreased to 170 AU in Case 2 from 250 AU for Case 1. Thus for these parameters, the size of the heliosphere has decreased by about 32% due to the plasma-neutral interaction. The VLISM flow is supersonic in these cases, and both have bow shocks visible in the top pane] of Fig. 1 (located at about 400 AU in Case 1 and about 300 AU in Case 2.)

It can be seen in the middle panel of Fig. 1 that the ldasrna-neutral interaction in Case 2 has caused the solar wind velocity to drop from 450 kin/s to shout 3$5 km/s inside the termination shock.

The distance to the termination shock is determined by a balance of solar wind and VLISM pressures

$$R_s \propto \sqrt{\frac{P_{ram,sw}}{P_{tot,vlism}}}.$$

A decrease from 450 to 385 km/s would cause a 14% decrease in the distance to the termination shock versus the 32% decrease observed. The somewhat larger effect is, surprisingly, the increase in the VLISM plasma ram pressure in front of the heliopause due to the acceleration of the plasma by the neutrals which are not directly slowed and diverted around the heliosphere at the nose. This has been verified by computing the total VLISM pressure $P_{tot,vlism}$ along the upstream symmetry axis. If there were no coupling to the neutrals, $P_{tot,vlism}$ would be constant from the outer boundary to the nose. In Case 2, however, we observe that $P_{tot,vlism}$ rises by 60% between the the injection boundary and the nose. These two neutral-plasma interaction effects, the deceleration of the solar wind plasma and the acceleration of the VLISM plasma, account for the observed 32% decrease in the size of the heliosphere.

The loss of neutral momentum to the VLISM plasma component as the flow approaches the nose leads to a pile up of neutrals in the region between the bow shock and the heliopause which can be sewn in the bottom panel of Fig. 1. This pile up, observed in the modeling results in B&M and *Baranov et al. (1991),* was descriptively termed a hydrogen "wall" in *Hall et* al. (1993). Comparison with the Case 2 density profile in the top panel shows that the neutrals abruptly increase in density by a factor of 2 just past the bow shock where the plasma flow has been decreased by the shock. Such a pile-up would affect the distribution of scattered Ly α light (*Baranov et al.*, 1991) and lead to an asymmetry in the upwind and downwind directions as observed by spacecraft (*Hall et al.*, 1993).

Simulation Results for a One Shock Heliosphere

For Cases 1 and 2, the Mach number of the inter stellar flow was M= 2.2 and bow shocks formed upstream of the leading edge of the heliopause in the simulations. We have also run a case with a higher VLISM temperature for both the neutrals and the plasma (T_{vlism} = 5 x 10^4 K, Case 3), making the VLISM flow subsonic (M= 0.96). The factor of 5 increase in temperature is used to mimic the effect of a VLISM field of about 0.3 nT in making the magnetosonic speed faster than the VLISM flow. All other parameters are as in Case 2.

In this subsonic VLISM flow case, the bow shock disappears as shown by the density profile in the second panel of Fig, 2 (Case 3, solid line). The lack of a bow shock has a dramatic effect on the distribution of neutrals ahead of the nose. In Case 3, no abrupt "hydrogen wall" is present. The neutral profile (top panel, Fig. 2) shows a gradual rise in neutral density from 0.14 to 0.13 cm^{-3} *as* opposed to the abrupt increase to 0.3 cm-3 seen in Case 2 (bottom panel, Fig. 1). The difference in the neutral distribution at the nose for heliospheres with and without a bow shock can be expected to cause a difference in the distribution of scattered solar Ly α light. Note that there is still a substantial gradient in the neutral density across the heliosheath; this would also lead to an upwind/downwind asymmetry in the distribution of Ly α radiation as observed (*Hall et al.*, 1993).

Also shown in the second panel of Fig. 2 is the density profile for a case with the parameters of Case 3 hut with no neutrals (Case 4, dashed line). The heliopause for Case 4, located at about 205 AU, is closer than in Case 1 because of the increase in the VLISM temperature by a factor of 5. In Case 3, the heliopause is at about 140 AU, for about a 30% decrease in the size relative to Case 4. Here, the the dominant effect in reducing the size of the heliosphere is the increase in $P_{tot,vlism}$ at the nose of the heliosphere resulting from the acceleration of the interstellar plasma by the neutrals as discussed ahove. The rise in $P_{tot,vlism}$ in Case 3 between the upstream simulation boundary and the heliopause accounts for about a 23% reduction in the size. By comparison, the decrease in the solar wind velocity inside the termination shock, from 450 to about 400 km/s, would by itself cause only about a 10% decrease.

Effects of Neutrals on Interplanetary Shock Propagation Time

In 1992, an extended 2-3 kHz radio emission event was observed at both Voyager 1 and 2 spacecraft (*Gurnett et al.*, 1993). These were similar to emission events reported earlier; the emission is presumably generated at f_p or $2f_p$ by electrons at the shock front (*Kurth et al.*, **1984).** Gurnett *et al.* proposed that these events resulted from the interaction of large interplanetary shocks (or a merged interaction region) with the heliopause; the shock was thought to be generated by the period of intense solar activity in late May and early June 1991. If these solar events were the cause, then the transit time of the shock from the sun to the heliopause was about 408 days. *Steinolfson and Gurnett* (1995, hereafter S&G) modeled the propagation of an interplanetary shock to the heliopause using a time-dependent two-dimensional fluid model. They found that they could match the 408 day transit time using a shock with a speed of 400 km/s relative to the solar wind and with solar wind parameters at Earth of $n_p = 5$ cm^{-3}, $v_{vsw} = 400$ km/s and $T_p = 2 \times 10^5$ K and VLISM parameters of $n_p = 0.09$ cm^{-3}, $T_p = 2 \times 10^4$ K and $v_{vlism} = 25$ km/s. The high interstellar density was needed to bring the heliopause in to 156 AU to match the 408 day transit time. However, S&G noted that an interstellar density of 0.09 cm^{-3} has a cutoff frequency of f_p = 2.7 kHz, well above the 1,8 kHz lowest frequency of the observed spectra. A cutoff frequency of 1.8 kHz corresponds to an interstellar plasma density of $n_p = 0.04$ cm^{-3}. If the emission were generated at the heliopause and if the observed 1.8 kHz corresponds to the plasma frequency of the interstellar plasma, then S&G concluded that there must be a magnetic field of about 4 nT to increase the VLISM pressure $P_{tot,vlism}$ sufficiently to bring the heliopause in to 156 AU.

We have repeated the computations of S&G, but now using our hydrodynamic model with the neutral-plasma interaction included in the simulations. We find that by including the plasma-neutral interaction, the distance to the heliopause can be made consistent with the approximately 408 day transit time when the VLISM plasma density has a cutoff frequency consistent with the observations using a reasonable value for the interstellar neutral density. For this simulation, Case 5, solar wind parameters and VLISM temperature and velocity were as in S&G (given above), except we have used a VLISM plasma density of 0.04 cm^{-3} as required to match the 1.8 kHz cutoff frequency. The neutral density used in the Case 5 calculation was n_N = 0.14 cm^{-3} which is within the range given by *Frisch* (1994). Figure 3 shows the contour plots for the plasma and neutral densities for this case. The VLISM flow is supersonic; the density contour plot shows a bow shock and the neutral contour plot shows the "hydrogen wall" as expected. Figure 4 shows the density profile at several times as the shock propagates to the heliopause. The shock moves rapidly up to the termination shock ($\approx 800\ km/s$), but slows dramatically in the heliosheath. Note from Fig. 4 that the VLISM density at the nose is about 0.1 cm^{-3} corresponding to a plasma frequency of 2.8 kHz which is comparable to the highest frequencies observed in this emission event.

Thus we conclude that, when the reduction in heliosphere size due to neutral-interaction is included, the shock transit time aud upper and lower emission frequencies can be made consistent with the observations, supporting the hypothesis in *Gurnett et al.* (1 993).

Discussion

Hydrodynamic simulation results were presented illustrating the effects of interstellar neutrals on the size of the heliosphere aud the distribution of neutrals at the heliosphere boundaries. The neutrals inter-act with the interstellar aud solar wind plasmas via charge-exchange collisions. Heliospheres with and without an external bow shock, corresponding to supersonic and subsonic VLISM plasma flow respectively, were modeled. For supersonic VLISM flow, a large pile up of neutrals was seen in the region between the bow shock and heliopause in the simulations. No such "hydrogen wall" was seen in the subsonic VLISM case. Both cases show a gradient in neutral density across the heliosheath. The difference in the neutral distribution aud density at the nose for heliosphere with and without a bow shock can be expected to cause different distributions of scattered solar Ly α light. Thus EUV observations from spacecraft such as Voyager and Pioneer (see *Hall et* al., 1993) may be able to determine whether or not the heliosphere has a bow shock. This, in turn, may give some indication of the strength of the VLISM magnetic field which cannot be measured if estimates of the interstellar plasma and neutral densities can be further refined.

Simulation results were also presented for modeling the propagation of a large interplanetary shock as a possible trigger for the Voyager 2-3 kHz emission events (*Gurnett et al.*, 1993). **Previous** hydrodynamic modeling efforts by *Steinolfson and Gurnett* (1995) had not be able to reconcile the size of the heliosphere (as determined from the shock transit time) with an interstellar density of $n_p = 0.04 cm^{-3}$ (inferred from the 1.8 kHz emission cutoff frequency). We are able to reconcile these by including the reduction in the size of the heliosphere due to the charge-exchange coupling with the interstellar neutrals. The VLISM neutral density needed was $n_N = 0.14$ cm-" 3 within the Currently excepted range (*Frisch*, 1994). 'J'bus, these results supports the hypothesis of *Gurnett et al.*, but uncertainties and unexplained features, such as the rising tones of the emissions, still remain.

Acknowledgements

This work was supported in part by NASA/Heliospheric Physics and in part by the NSF Center for Research in Parallel Computation under Cooperative Agreement CCR-88809615. A portion of this work was carried out at the Jet I'repulsion Laboratory, California Institute of Technology, under a contract with NASA. The JPL/Caltech CRAY YMP and T3D used in this investigation was supported by NASA.

References

V. B. Baranov and Yu G. Malama, Model of the Solar Wind Interaction with the Local Interstellar Medium: Numerical Solution of Self-Consistent Problem, *J. Geophys.* Res. 98, 15157, 1993.

V. B. Baranov, M. G. Lebedev, and Yu G., The Influence of the Interface between the Heliosphere and the Local Interstellar Medium on the Penetration of H atoms to the Solar System, *Astrophys. J.* 375, 347, 1991.

P. C. Frisch, Morphology and Ionization of the Interstellar Cloud Surrounding the Solar System, Science, 265, 1423, 1994.

D. A. Gurnett, W, S. Kurth, S. C. Allendorf, and R. L. Poynter, Radio Emission from the Heliopause Triggered by an interplanetary Shock, *Science* 262, 199, 1993.

D. T. Hall, D. E. Shemansky, D. L. Judge, P. Gangopadhyay, and M. A. Gruntman, Heliospheric Hydrogen beyond 15 AU: Evidence for a Termination Shock, *J. Geophys. Res.* 98, 15185, 1993.

T. E. Holz teraction of the Solar Wind with the Neutral Component of the Interstellar Gas, *J. Geophys. Res.* 77, 5'107, 19'72.

Karmesin, S. R., P. C. Liewer, J. U. Brackbill, Two-dimensional Simulations of the Motion of the Termination Shock in Response to an 11 Year Variation in the Solar Wind, *Geophys. Res. Lett.* **22, 1153,** 1995.

W. S. Kurth, D. A. Gurnett, 11'.1. Scarf, and R. L. Poynter, Detection of a radio emission at **3** kHz in the Outer Heliosphere, *Nature* 312, 27, 1984.

H. 1,. Pauls, G. P. Zank and 1,. L. Williams, Interaction of the Solar Wind with the Local Interstellar Medium, *J. Geophys. Res.* in press, 1995.

R. S. Steinolfson and D. A. Gurnett, Distances to the Termination Shock and Heliopause from a Simulation Analysis of the 1992-93 Heliospheric Radio Emission Event, *Geophys. Res. Lett.* 22, 651, 1995.

Figure 1. Simulation results for Case 1 (dashed line) without neutrals and Case 2 (solid line) with neutrals showing the reduction in the size of the heliosphere due to plasma-neutral charge-exchange interactions. Profiles are along an upstream line through the nose of the heliosphere ($\theta = 0$). The top and middle panels compare the density and velocity profiles respectively. The VLISM flow is supersonic; note the presence of a bow shock in both cases. The bottom panel is the neutral profile for Case 2 showing the build up of hydrogen at the leading edge of the heliopause.

Figure 2. Simulation results for Case 3 (solid line) with neutrals and Case 4 (dashed line) without neutrals for subsonic VLISM flow. The top panel shows the neutral profile for Case 3 and the bottom panel compares the density profiles. No bow shock is seen. A similar reduction in the size of the heliosphere is seen for this subsonic case as *for the supersonic* VLISM case in Fig. 1. However, no build up of neutral hydrogen is seen at the leading edge of the heliopause.

Figure 3. Contour plots of the plasma (top) and neutral (bottom) densities for the equilibrium of Case 5. An interplanetary shock of speed 400 km/s relative to the solar wind was launched into this equilibrium at the inner boundary. The VLISM plasma density is n_p = 0.04 cm^{-3} consistent with the 1.8 kHz lowest frequency of the Voyager emission events. A neutral density of n_N = 0.14 cm^{-3} has brought the heliopause in to about 150 AU. Note the "hydrogen wall" in the neutral density contour plot which forms between the bow shock and the heliopause.

Figure 4. Case 5 plasma density profiles at three times along the $\theta = 0$ line showing the propagation of the interplanetary shock (the density bulge) to the heliopause. The propagation time was about 400 days, consistent with the time estimate in Gurnett et al (1993) for the IP shock which may have triggered the Voyager 2-3 kHz emission event. The highest plasma density, at the stagnation point of the VLISM flow, is $n_p \approx$ 0.1 cm-3 corresponding to $f_p = 3\ kHz$, about the highest frequency seen in the emission event.

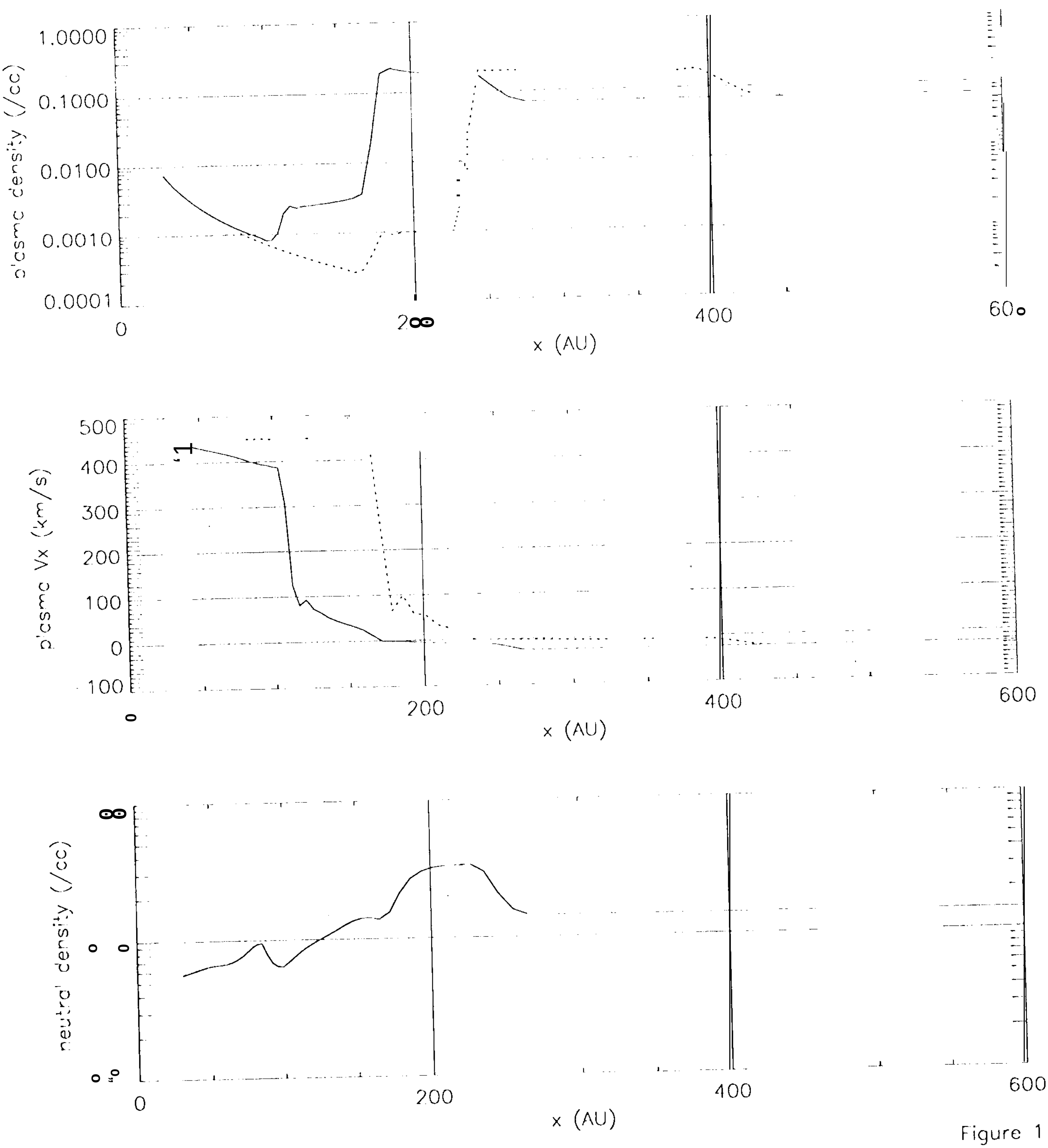
plasma density (/cc)
1.0000
0.1000
0.0100
0.0010
0.0001
0
200
400
600
x (AU)
plasma Vx (km/s)
500
400
300
200
100
0
-100
x (AU)
neutral density (/cc)
x (AU)

Figure 1

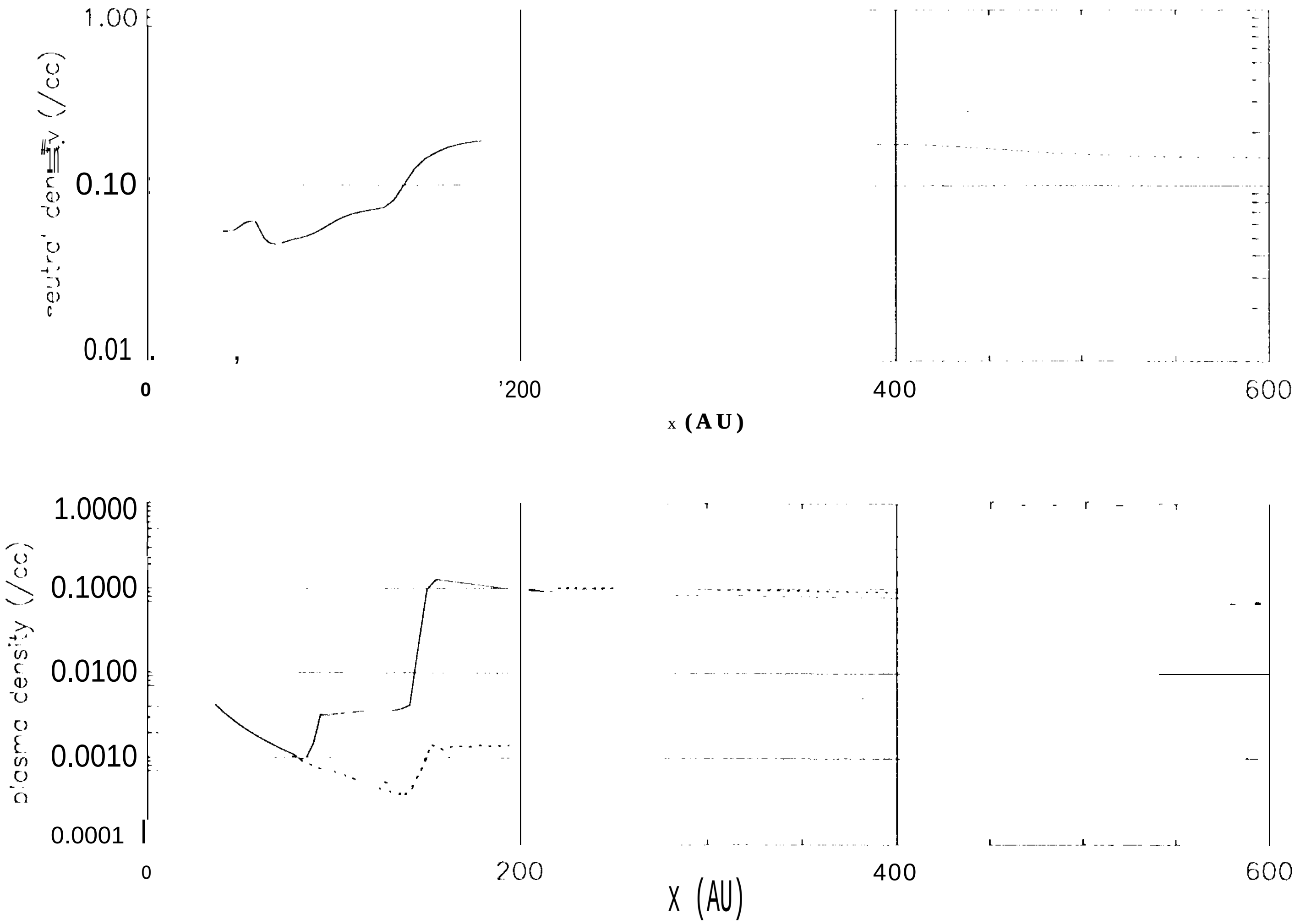

1.00
0.10
0.01
neutral density (/cc)
0
200
400
600
x (AU)
1.0000
0.1000
0.0100
0.0010
0.0001
plasma density (/cc)
0
200
400
600
X (AU)

Figure '2

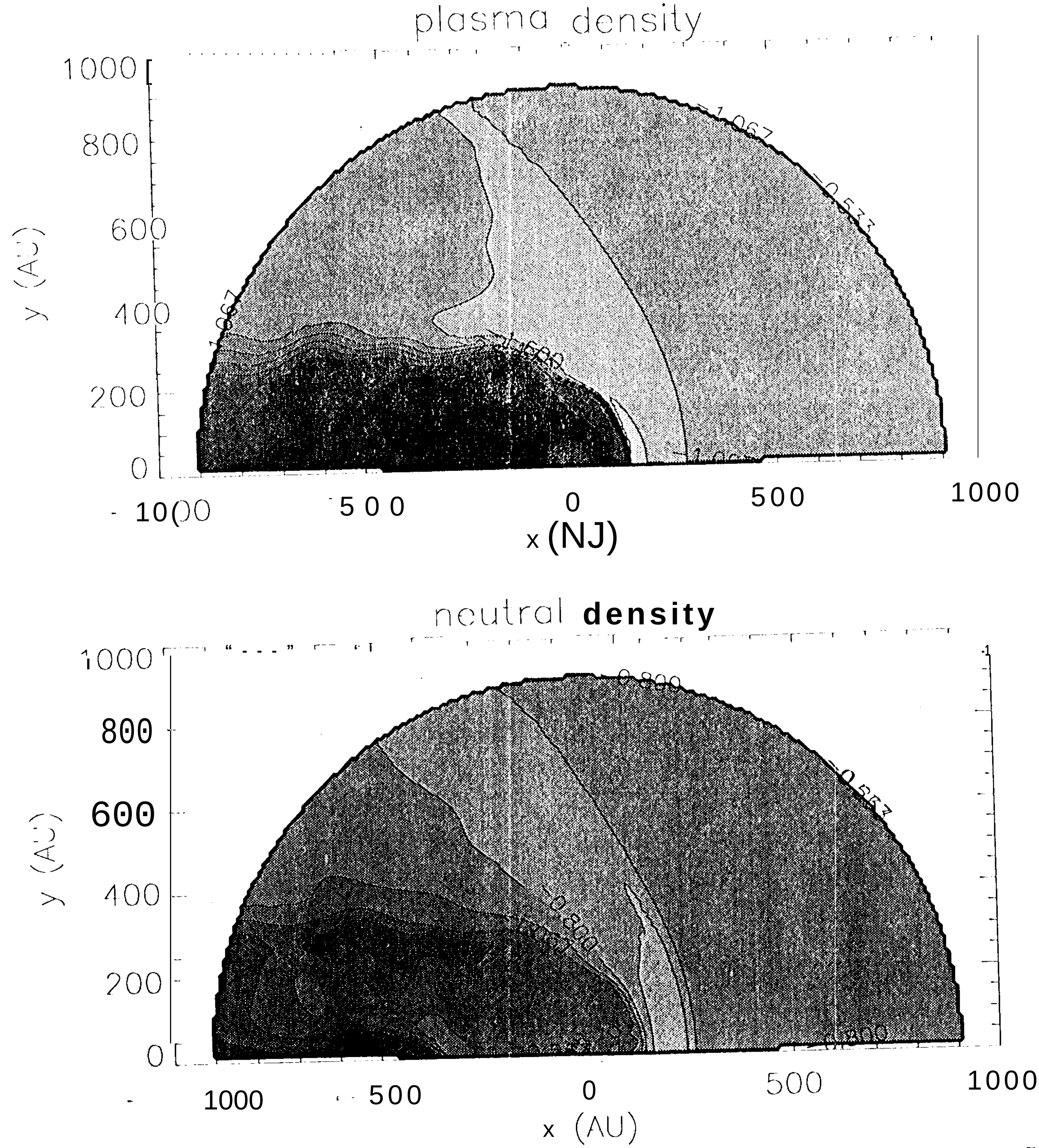
plasma density
1000
800
600
400
200
0
y (AU)
-1000
-500
0
500
1000
x (NJ)
1.067
0.533
neutral density
1000
800
600
400
200
0
y (AU)
-1000
-500
0
500
1000
x (AU)
0.800
0.533

Figure 3

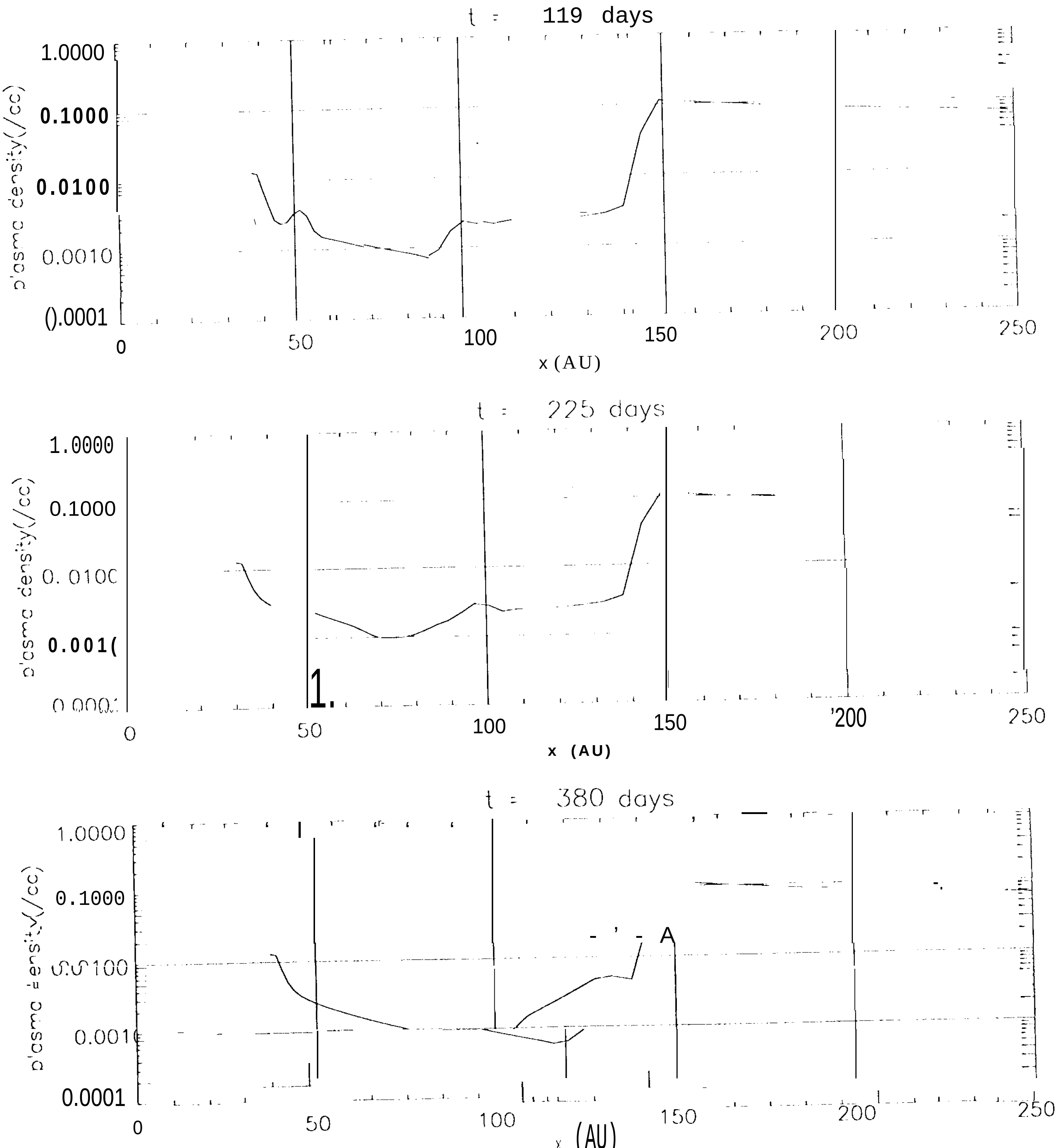
t = 119 days
plasma density(/cc)
1.0000
0.1000
0.0100
0.0010
0.0001
0
50
100
150
200
250
x (AU)
t = 225 days
plasma density(/cc)
1.0000
0.1000
0.0100
0.0010
0.0001
0
50
100
150
200
250
x (AU)
t = 380 days
plasma density(/cc)
1.0000
0.1000
0.0100
0.0010
0.0001
0
50
100
150
200
250
x (AU)

Figure 4